Deep Space Network

210
Delta Differential One-way Ranging

Document Owner:		Approved By:	
Signature Provided	11/30/2020	Signature Provided	12/22/2020
James S. Border	Date	Timothy Pham	Date
Delta-DOR System Engineer		Communications Systems Chief Engineer	
Prepared By:		Released by:	
Signature Provided	01/04/2021	Signature Provided	02/05/2021
Dong Shin	Date	Christine Chang	Date
DSN System Engineer		DSN Document Release Authority	

Review Acknowledgment

By signing below, the signatories acknowledge that they have reviewed this document and provided comments, if any, to the signatories on the Cover Page.

Signature Provided	12/01/2020	Signature Provided	12/01/2020
Jeff Berner	Date	Alina Bedrossian	Date
DSN Project Chief Engineer		Science System Engineer	

Document Change Log

Rev	Issue Date	Prepared By	Affected Sections or pages	Change Summary
Initial	07/15/2004	P. W. Kinman	All	New Module
A	02/09/2015	A. Bedrossian J. S. Border D. Shin	All	Replaced description of VSR with description of WVSR. Added DSS-35 interface. Updated error budget.
B	02/10/2017	J. S. Border D. Shin	Section 2	Add DSS-36 interface. Remove DSS-45 interface.
C	06/06/2019	J. S. Border	Section 2	Replaced description of WVSR with description of OLR in Section 2.1. Updated stations shown in Fig. 2. Updated error budget in Section 2.5.
D	02/05/2021	A. Bedrossian J. S. Border D. Shin	Figure 2	Added DSS-53 and DSS-56. Added DSS-65 decommission date.

Contents

Illustrations

Tables

Table   **Page**

1 Introduction

1.1 Purpose

This module describes the capabilities and identifies the performance parameters for Delta-Differential One-way Ranging (ΔDOR) measurements at the Deep Space Network (DSN) 34-m and 70-m stations.

1.2 Scope

The document provides information on the Delta-Differential One-way Ranging (ΔDOR) technique. This document describes those parameters and operational considerations that are independent of the particular antennas being used. For antenna-dependent parameters, refer to the appropriate telecommunications interface module in DSN Document 810-005, modules 101, 103 and 104 of this handbook. The interpretation of any particular ΔDOR measurement is dependent on the precise locations of the tracking antennas. Station locations are provided in module 301, Coverage and Geometry. ΔDOR signals are received by the Open Loop Receiver (OLR). The quality of a ΔDOR measurement depends in part on solar wind velocity that is discussed in module 106, Solar Corona and Solar Wind Effects. Modules of 810-005 that cover DSN capabilities related to ΔDOR are listed in Appendix A.

2 General Information

Delta-Differential One-way Ranging is a radio-tracking technique that has proved very useful in the orbit determination of some spacecraft (References 1 and 2). A comprehensive review of ΔDOR development in the DSN is given in Reference 3. A comprehensive technical description including fundamentals, design trade-offs, and performance is given in Reference 4. Delta-DOR is an interferometric technique and therefore requires two Deep Space Stations located at different complexes for a single measurement.

2.1 Description of the Measurement

ΔDOR uses the differential one-way range technique to provide information about the angular location of a target spacecraft relative to a reference direction where the reference direction is defined by the direction of arrival of radio waves from a source whose direction is well known. This is the origin of the "Δ" in the name "ΔDOR". The term *reference source* is applied to the distant source of radio waves that define the reference direction. Typically, the reference source is a quasar whose angular position in the sky is well known and cataloged, having been previously measured and studied. Sometimes, the reference source is a second spacecraft whose position in the sky is better known than that of the target spacecraft.

DSN Document 810-005, Module 107 contains the current X-band radio source catalog. Work is in progress to publish the Ka-band radio source catalog as module 108. For further information on radio source catalog development, see References 5 and 6.

Since ΔDOR provides a direct geometric determination of spacecraft angular position, it is especially useful for cases where line-of-sight measurements have weaknesses such as spacecraft near zero declination and spacecraft with small, unmodeled dynamic forces affecting their motion. It can also provide an independent cross-check of orbits determined by other methods and, in combination with these methods, can improve the accuracy of trajectory determination. Further, ΔDOR measurements are of relatively short duration when compared to other orbit determination methods such as Doppler and two-way ranging (typically one hour or less compared with many hours). Thus, they can be used to reduce the total amount of tracking time necessary to attain the desired level of trajectory accuracy. The main disadvantages of ΔDOR are that it requires two stations for each measurement and, in most cases, will disrupt telemetry when the reference source is being viewed.

2.1.1 *Differential One-Way Ranging*

The name, differential one-way ranging, comes from the fact that only a range difference, rather than an absolute range, is determined and that only the downlink is used. It is because only a range difference is being measured that it is possible to make this measurement one-way. (Absolute range measurement requires a highly-accurate clock at the target spacecraft as any clock error would translate directly into a range measurement error. This is the reason that ordinary ranging measurements send a ranging code derived from the station clock to the spacecraft, see modules 203 and 214.)

The geometry of differential one-way range is depicted in Figure 1. The radio waves from the target spacecraft arrive in approximately parallel rays at the interferometer. An imaginary line that connects the two antennas forming the interferometer is called the baseline and is denoted B in Figure 1. Since the antennas of the interferometer are located in different complexes on separate continents, the baseline B passes through the Earth. Also in Figure 1, an imaginary line segment L is drawn that is perpendicular to the arrival direction of the incoming rays. The shaded area around L represents the *a-priori* uncertainty in angle A and, because L is perpendicular to R, the uncertainty of the angle of the incoming radio waves with respect to the baseline. The interferometer measures the path length difference, also known as differential one-way range and indicated as δR in the figure. This enables the accuracy of A to be significantly improved. It is important to note that this is not a complete solution for the angular position in the sky of the target spacecraft. A single measurement only provides information about the location of the target spacecraft in the plane defined by the interferometer baseline and the target spacecraft.

The path length distance (δR) is determined by recording the signals arriving at each station using an open-loop receiver. Later, when the signals from both stations are available at a common location, the two signals are correlated. The difference in group delay associated with the paths followed by the target spacecraft signal in propagating to the two stations is determined (τ_g) and converted into a path length difference by multiplying by the speed of electromagnetic waves in space (c). The path length difference and knowledge of the baseline orientation is used to refine the angular position of the of the target spacecraft in the sky. The errors inherent in the DOR and ΔDOR process are discussed in Paragraph 2.4 and summarized in

Paragraph 2.5. In discussing these errors, it is customary to use time units – that is, the units of differential group delay.
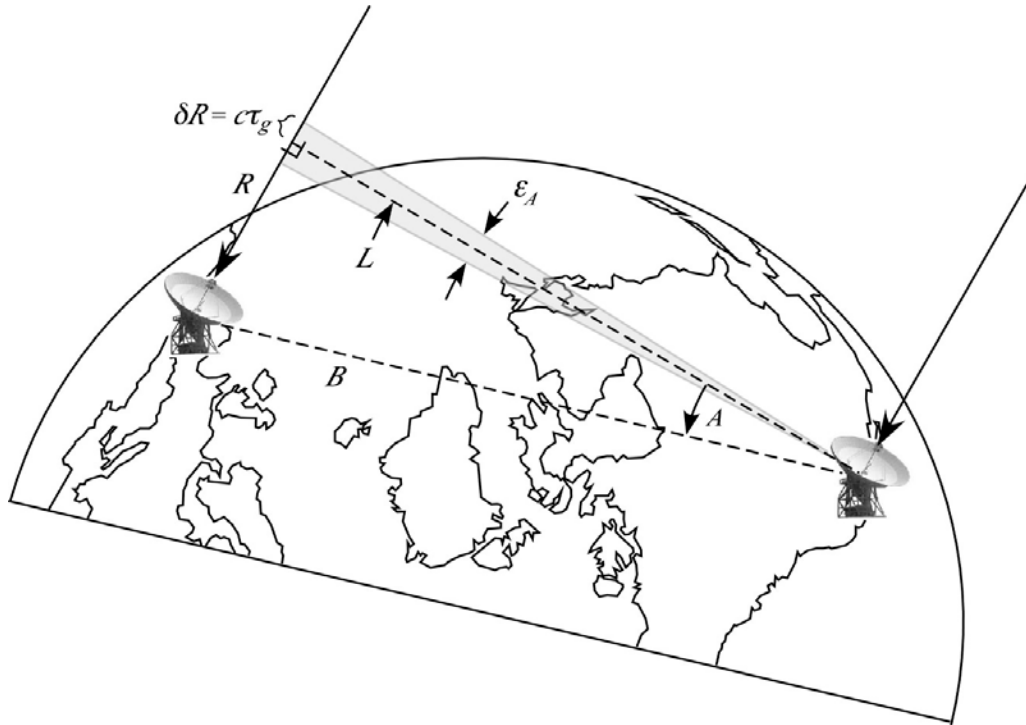

Figure 1. Geometry of Differential One-Way Ranging
(B = Baseline; L = perpendicular to incoming rays; A = angle between B and L;
δR = differential one-way range, ε_A = uncertainty in angle A)

      The signals transmitted by the spacecraft should be high frequency sinewave or pseudo-noise (PN) waveforms to provide the best precision. These signals are commonly referred to as "DOR Tones". Lower frequency subcarrier harmonics can be substituted for DOR tones, with some loss of precision, if DOR tones are not available. The subcarrier harmonics may be pure tones or spread by telemetry. The lowest possible symbol rate is preferred to reduce the squaring loss that occurs during signal processing. Uplinked range tones provide even less precision, but may be used if no other components are available. Subcarrier harmonics or additional DOR tones may also be required in order to resolve the phase ambiguity, see Paragraph 2.3

2.1.2   ΔDOR

      ΔDOR is a much more useful measurement for orbit determination than is plain DOR. In principle, a DOR measurement provides information about the angular position of the target spacecraft (within the plane of the interferometer plus target spacecraft). However, there are a number of measurement errors that prevent this form of measurement from being useful in

the solution of the typical deep space orbit determination problem. The sources of these measurement errors are (among others) station clock offsets, instrumental group delays, and media effects. To calibrate these effects, a plain DOR measurement is made on a reference source that is near the target spacecraft in an angular sense. The antennas are quickly moved to the target spacecraft and a similar measurement is made. Finally, the antennas are returned to the reference source to verify the calibration. This technique enables the effects of station clock offsets, instrumental group delay errors, and most of the media effects to be cancelled when the individual DOR results are differenced (which is a ΔDOR measurement). The result is that the errors in a ΔDOR measurement are much smaller than those for a plain DOR measurement and the technique becomes sufficiently accurate for orbit determination.

A number of missions have used ΔDOR measurements as part of their orbit determination. ΔDOR measurements played an important role in the orbit determination of 2001 Mars Odyssey (Reference 2) and the Mars Exploration Rovers (MER) (Reference 7). Those ΔDOR measurements were performed at X band. Delta-DOR measurements were also performed in the Ka band for the Mars Reconnaissance Orbiter using beam-waveguide stations (Reference 8). It should be noted that a VLBI measurement will always use two stations at different complexes; therefore stations 25 and 26 would not be used in the same measurement nor would stations 54 and 55.

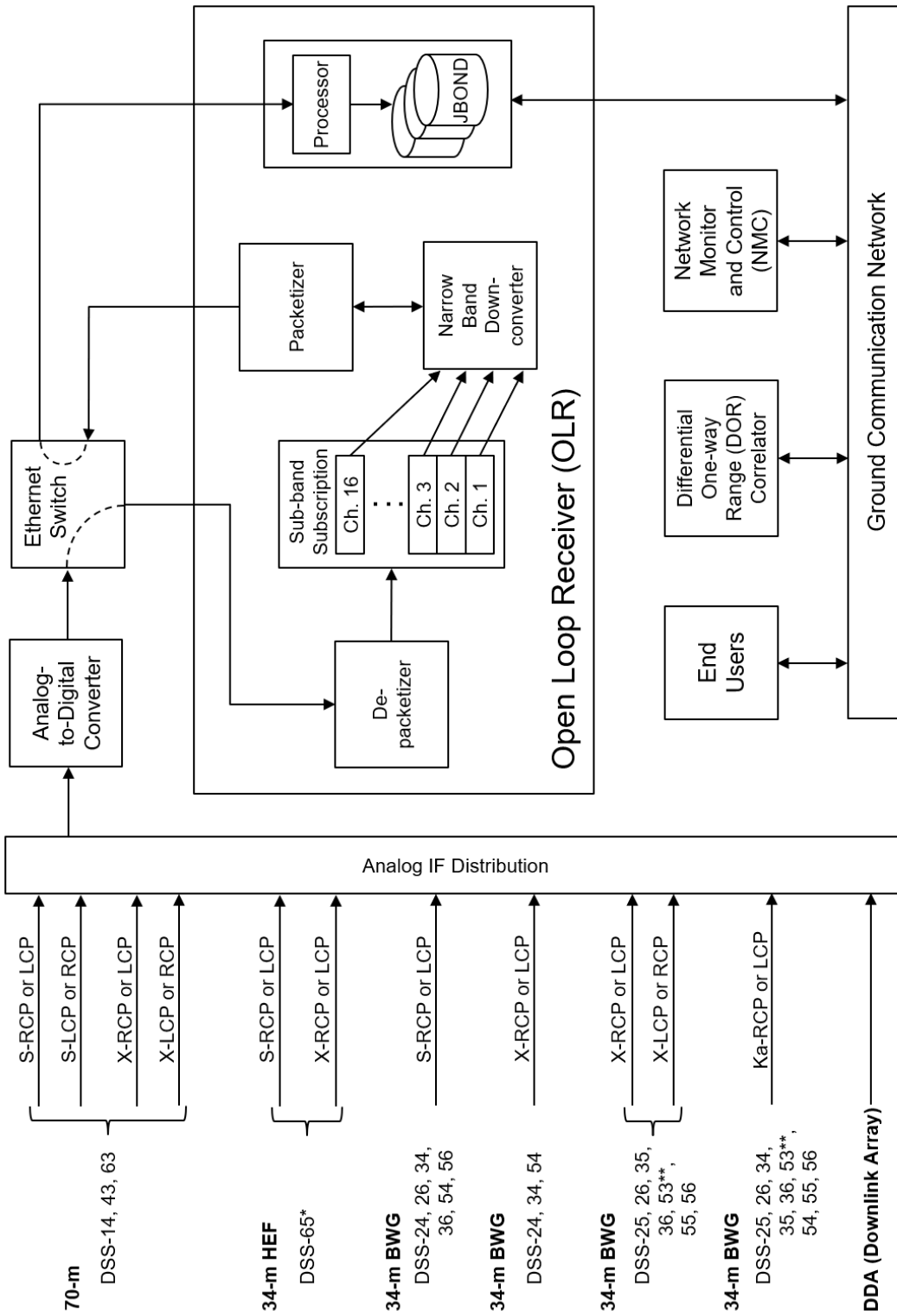### 2.1.3   DSN Equipment for ΔDOR Support

Differential one-way ranging is supported by the 34-m and 70-m antennas. Other equipment includes the OLRs in the complex Signal Processing Center (SPC), the ground communications infrastructure, and the DOR Correlators at Jet Propulsion Laboratory (JPL) and Goldstone Deep Space Communication Complex (GDSCC). Figure 2 depicts the DSN equipment used for ΔDOR support.

The input to the OLR is one or two digital Intermediate-Frequency (IF) signals that have been downconverted from the microwave sky frequency, also referred to as the radio frequency (RF). The IF signals cover the full usable signal bandwidth. The RF passbands are fixed and, in combination with the RF to IF downconverters, place restrictions on the frequency ranges in which the ΔDOR tones can be received. These restrictions, in terms of microwave sky frequency, are listed in Table 1. Additional restrictions based on the bandwidths of the antenna low noise amplifiers can be found in DSN Document 810-005, space link interfaces modules 101, 103, and 104.

Table 1. Microwave Sky Frequency Ranges for ΔDOR Tones

Band	Acceptable Frequency Range	Remarks
S-band	2,200–2,310 MHz	Deep Space Allocation is 2,290–2,300 MHz
X-band	8,200*–8,600 MHz	Deep Space Allocation is 8,400–8,450 MHz
Ka-band	31,800–32,300 MHz	Deep Space Allocation is 31,800–32,300 MHz

* DSS-35 X-band range is from 8,225 MHz-8,600 MHz

Figure 2. DSN Equipment for ΔDOR Support

The digital IF signals input to the OLR are in the range of 100 to 600 MHz. The OLR further downconverts and filters these IF signals to baseband channels for recording. Up to 16 baseband channels can be defined. The IF is downconverted to a specified center frequency and filtered to a specified bandwidth for each baseband channel. The downconversion can either be at a fixed frequency or can be optionally steered by predicts of the expected spacecraft sky frequency. Complex I/Q samples with 1 to 16 bit resolution are recorded. The supported bandwidths and sample resolutions are shown in Table 2. The OLR is capable of recording at other bandwidths also. Only the bandwidths and sample resolutions shown in Table 2 have been validated for use with the Delta-DOR processing system. The maximum aggregate record rate is 512 Mb/s.

Channels are typically defined for areas of interest that may include the carrier, the DOR tones and their harmonics, and harmonics of subcarriers. The composite data volume for all selected channels at each of the two stations involved in the measurement must be routed to one of the ΔDOR correlators at either JPL or GDSCC for processing. This is a large amount of data and the capability of the ground communications infrastructure is often a key factor in determining the overall time required to complete a ΔDOR measurement. At current effective transmission rates of about 80 Mb/s, (288 Gb/hr), the data from a typical one hour ΔDOR pass (32 minutes of six channels of 2-bit quantized quasar data with an 8 MHz bandwidth, and the associated narrower bandwidth channels for spacecraft signals), can be delivered to the correlator in about 1.3 hours.

Table 2. Supported Bandwidths and Resolutions with Resulting Data Rate

Type Filter	Bandwidth	Resolution (bits per sample)	Resultant Data Rate (b/s)
Narrowband	1 kHz	16	32,000
	2 kHz	16	64,000
	4 kHz	16	128,000
	8 kHz	16	256,000
	16 kHz	16	512,000
	25 kHz	16	800,000
	50 kHz	16	1,600,000
	100 kHz	16	3,200,000
	200 kHz	16	6,400.000
	500 kHz	16	16,000,000
	1 kHz	8	16,000
	2 kHz	8	32,000
	4 kHz	8	64,000
	8 kHz	8	128,000

Table 2. Supported Bandwidths and Resolutions with Resulting Data Rate (Continued)

Type Filter	Bandwidth	Resolution (bits per sample	Resultant Data Rate (b/s)
	16 kHz	8	256,000
	25 kHz	8	512,000
	50 kHz	8	800,000
	100 kHz	8	1,600,000
	200 kHz	8	3,200,000
	500 kHz	8	8,000,000
Wideband	1 MHz	8	16,000,000
	2 MHz	8	32,000,000
	4 MHz	8	64,000,000
	8 MHz	8	128,000,000
	16 MHz	8	256,000,000
	1 MHz	4	8,000,000
	2 MHz	4	16,000,000
	4 MHz	4	32,000,000
	8 MHz	4	64,000,000
	16 MHz	4	128,000,000
	32 MHz	4	256,000,000
	1 MHz	2	4,000,000
	2 MHz	2	8,000,000
	4 MHz	2	16,000,000
	8 MHz	2	32,000,000
	16 MHz	2	64,000,000
	32 MHz	2	128,000,000
	1 MHz	1	2,000,000
	2 MHz	1	4,000,000
	4 MHz	1	8,000,000
	8 MHz	1	16,000,000
	16 MHz	1	32,000,000
	32 MHz	1	64,000,000

2.1.4   Data Acquisition

ΔDOR measurements are conducted using either the Goldstone-Madrid baseline or the Goldstone-Canberra baseline. Two baselines with orthogonal components are needed to measure both the right ascension and declination coordinates of angular position. The Goldstone-Madrid baseline is oriented east-west and is most sensitive to right ascension for spacecraft near the ecliptic plane. The Goldstone-Canberra baseline is canted and has most sensitivity in the direction that splits the axes of right ascension and declination. Since declination is usually the most difficult component of spacecraft state to extract from line-of-sight measurements, the Goldstone-Canberra baseline may provide information that cannot otherwise be obtained. The Goldstone-Madrid baseline is still useful to evaluate small dynamic force modeling and improve overall trajectory accuracy.

Planning a measurement involves scheduling the stations, selecting DOR tones or signal frequencies to be used, and identifying the appropriate reference source(s). Each OLR can process up to 16 signal components. Spacecraft tones are typically recorded in narrow channels, while quasar noise and spacecraft PN signals must be recorded in wide channels.

Narrow channels range in bandwidth from 1 to 500 kHz. Sample resolution of 1 to 16 bits may be selected. Channels are centered on the predicted received frequency of the spacecraft signal component to be recorded. Channel bandwidth must be chosen wide enough to include margin for errors in prediction of the spacecraft transmitter frequency and Doppler shift. Enough bits should be used to protect against radio frequency interference and avoid loss of Signal-to-Noise ratio. The spacecraft data volume is usually much smaller than the quasar data volume. As a result, a wider bandwidth or greater sampling resolution may be selected for the narrow channels without significantly increasing the total amount of data.

Quasar channels range from 1 to 32 MHz. A sample resolution of 1 to 2 bits is usually selected. Channel bandwidth must be chosen wide enough to provide sensitivity to detect the faint signals from extra-galactic radio sources that are used to calibrate the DSN as an interferometer. A channel bandwidth of 8 MHz with 2 bit samples is adequate to detect a significant number of the sources in the JPL radio source catalog using a pair of DSN 34m antennas. A narrower bandwidth may be selected, and only stronger quasars observed, in order to reduce the volume of data that must be recorded.

To perform a measurement, the two Deep Space Stations forming the very long baseline interferometer make a series of observations to determine the differential one-way range to the target spacecraft and the reference source(s) that preferably has a small angular separation from the target spacecraft. (Differential one-way ranging with a quasar is similar to what has been described above for a target spacecraft; however, there are important differences since the nature of the quasar "signal" is quite different from that of a spacecraft with DOR tones.) Each observation is referred to as a *scan*. In a typical ΔDOR tracking pass of approximately one hour, the spacecraft and reference are alternately observed and a total of 5 to 10 scans, each lasting 5 to 10 minutes, are typically recorded. Some sources of measurement error can be reduced by making more observations, using shorter scans, and by more frequent switching between spacecraft and quasar. Only a slight improvement in the overall measurement accuracy can be obtained by increasing the measurement time beyond 1 hour in order to repeat the observations.

The following four scenarios are provided as examples of typical ΔDOR measurements made by the DSN.

2.1.4.1   *Example 1, Spacecraft With One DOR Tone and Subcarrier Harmonics*

- Tone frequency: 19.1 MHz

- Subcarrier frequency: 375 kHz

- Number of channels: 6 spacecraft and 6 quasar

- Narrow channel bandwidth: 50 kHz sampled with 8-bit resolution

- Wide channel bandwidth: 8 MHz sampled with 2-bit resolution

Table 3. Channel Assignments for Example 1

Channel	Spectral Component
1	Carrier
2	Upper 3rd harmonic of subcarrier
3	Lower 1st harmonic of DOR tone
4	Upper 1st harmonic of DOR tone
5	Lower 2nd harmonic of DOR tone
6	Upper 2nd harmonic of DOR tone

2.1.4.2   *Example 2, Two Spacecraft With One DOR Tone and Subcarrier Harmonics*

- Tone frequency: 19.1 MHz

- Subcarrier frequency: 375 kHz

- Number of channels: 4 for each spacecraft and 8 quasar

- Narrow channel bandwidth: 50 kHz sampled with 8-bit resolution

- Wide channel bandwidth: 2 MHz sampled with 2-bit resolution

Table 4. Channel Assignments for Example 2

Channel	Spectral Component
1	Carrier of spacecraft 1
2	Carrier of spacecraft 2
3	Upper 3rd harmonic of spacecraft 1 subcarrier
4	Upper 3rd harmonic of spacecraft 2 subcarrier
5	Lower 1st harmonic of spacecraft 1 DOR tone
6	Lower 1st harmonic of spacecraft 2 DOR tone

| 7 | Upper 1st harmonic of spacecraft 1 DOR tone |
| 8 | Upper 1st harmonic of spacecraft 2 DOR tone |

2.1.4.3   *Example 3, Spacecraft With Only Subcarrier Harmonics*

- Subcarrier frequency: 262 kHz

- Number of channels: 4 spacecraft and 4 quasar

- Narrow channel bandwidth: 50 kHz sampled with 8-bit resolution

- Wide channel bandwidth: 2 MHz sampled with 2-bit resolution

Table 5. Channel Assignments for Example 3

Channel	Spectral Component
1	Carrier
2	Lower 30th harmonic of subcarrier
3	Upper 26th harmonic of subcarrier
4	Upper 30th harmonic of subcarrier

In practice, squarewave subcarriers with finite risetimes have discrete spectral lines at the even harmonics of the subcarrier frequency whereas the odd harmonics may have data modulation. Therefore, even harmonics may be better choices for ΔDOR assuming they have sufficient power. It also may be necessary to select even harmonics if the telemetry symbol rate cannot be reduced sufficiently to be processed by the ΔDOR correlator.

2.1.4.4   *Example 4, Spacecraft With Uplinked Range Tone*

- Range Tone frequency: 1 MHz

- Number of channels: 3 spacecraft and 3 quasar

- Narrow channel bandwidth: 50 kHz sampled with 8-bit resolution

- Wide channel bandwidth: 2 MHz sampled with 2-bit resolution

Table 6. Channel Assignments for Example 4

Channel	Spectral Component
1	Carrier
2	Lower 1st harmonic of range tone
3	Upper 1st harmonic of range tone

2.2   *Downlink Signal Structure and Power Allocation*

The target spacecraft may use one or two DOR tones, phase-modulated onto the downlink carrier, for a ΔDOR measurement. For sinusoidal DOR tones, the mathematical form of the downlink carrier may generally be modeled as

$$\sqrt{2P_T}\,\sin\!\left[\,2\pi f_c t + \theta d(t) + \theta_1 \sin\!\left(2\pi f_1 t\right) + \theta_2 \sin\!\left(2\pi f_2 t\right)\right] \tag{1}$$

where P_T is the total downlink power, f_c is the carrier frequency, $d(t)$ is the telemetry and θ its modulation index. The DOR tones will have frequencies f_1 and f_2, and modulation indices of θ_1, and θ_2 if two tones are present, however the second DOR tone will sometimes be absent.

A detailed description of spacecraft signal structure used for ΔDOR observations is given in Section 3.2 of Reference 4.

Recommendations for DOR modulation are given in Reference 9. The recommendations include the number of DOR tones, DOR tone frequency, and DOR tone power.

2.3   *DOR Tones and Phase Ambiguity*

For each DOR tone that phase-modulates the downlink carrier, an upper and a lower fundamental harmonic are created. Thus, a (differential) group delay can be measured even when only one DOR tone modulates the carrier. However, it is sometimes advantageous to have two DOR tones. The DOR tones will normally be coherently related and may be coherently related to the carrier. Furthermore, if carrier-aided detection is to be used, the DOR tones must be coherently related to the carrier (Reference 9). If a DOR tone of about 20 MHz is used in the X band, then it is preferred for the downlink carrier to be assigned a channel near the center of the allocated band, in order that the upper and lower fundamental harmonics of the DOR tone lie within the allocated band.

When two DOR tones are present, the purpose of the additional DOR tone is to resolve the phase ambiguity that is inherent in any range (or differential range) measurement. For example, in two-way sequential ranging, the phase ambiguity associated with the range clock is resolved by sequentially sending a set of range components of decreasing frequency, see 810-005, module 203. With differential one-way ranging, the DOR tones are sent simultaneously rather than sequentially.

In order to make clear why two DOR tones are sometimes necessary, it is well to consider first the case of a single DOR tone. Corresponding to the single DOR tone, there are two fundamental harmonics (an upper and a lower). After each harmonic has been downconverted and recorded at the two stations, the differential phase between the two received copies of each harmonic may be plotted as indicated in Figure 3. The abscissa is the frequency of the observed harmonic as recorded at intermediate frequency. The ordinate is the differential phase. The column of points on the left side of Figure 3 represents the differential phase for the lower fundamental harmonic. The column of points on the right side of Figure 3 represents the differential phase for the upper fundamental harmonic. The horizontal separation between the

two columns of points is the spanned bandwidth, which equals twice the frequency of the DOR tone. The slope of the line labeled "True" is the differential group delay for the DOR tone.
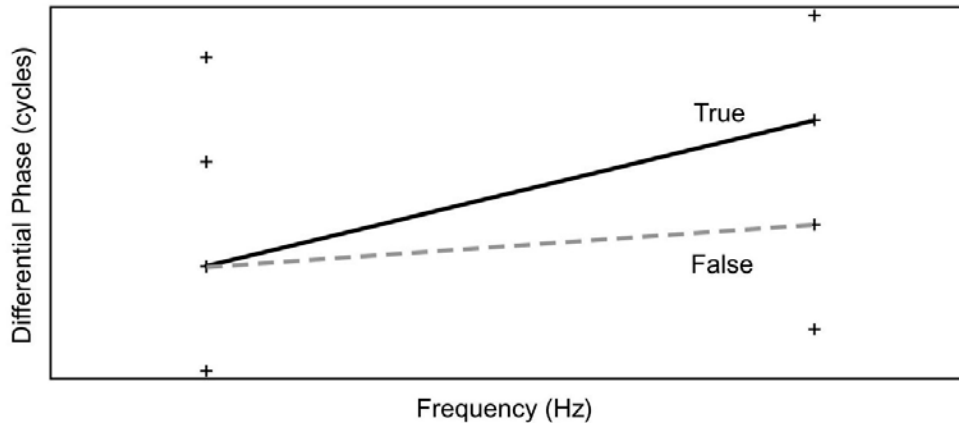

Figure 3. Phase Ambiguity with One DOR Tone

In Figure 3, there is a phase ambiguity since the DOR tone is a periodic signal. If the differential phase is regarded as having an integer number of cycles plus a fraction of one cycle, differential one-way ranging only measures the fractional part. That is why there is a column of points for the lower fundamental harmonic (and also for the upper fundamental harmonic). The points in each column are spaced by one cycle of phase. For the purpose of a ΔDOR measurement, it is not necessary to determine which point in the first column of points represents the true differential phase for the lower fundamental harmonic. However, it is necessary to distinguish the true slope, representing the actual differential group delay, from the false slope shown as a dashed line in Figure 3. The difference between these two slopes equals the reciprocal of the spanned bandwidth. (There are other false slopes than the one shown in Figure 3, but these other false slopes have a value at least as far from the true slope as the reciprocal of the spanned bandwidth.) If the *a priori* knowledge of the differential group delay is good enough to rule out a false slope corresponding to a delay that differs from the true differential group delay by the reciprocal of the spanned bandwidth, then there is no need for a second DOR tone.

Figure 4 illustrates how differential group delay is determined when there are two DOR tones. The leftmost column of Figure 4 represents the differential phase for the lower fundamental harmonic of the higher-frequency DOR tone. The rightmost column represents the differential phase for the upper fundamental harmonic of the higher-frequency DOR tone. The middle columns represent differential phase for the lower and upper fundamental harmonics of the other (lower-frequency) DOR tone. The horizontal separation between the two outermost columns of points is the spanned bandwidth, which equals twice the frequency of the higher-frequency DOR tone. The true and false slopes shown in Figure 3 are reproduced in Figure 4. It is now clear how the second (lower-frequency) DOR tone helps resolve phase ambiguity. The

true slope passes through legitimate points in the middle columns, whereas the false slope does not. On this basis, the false slope can be ruled out.
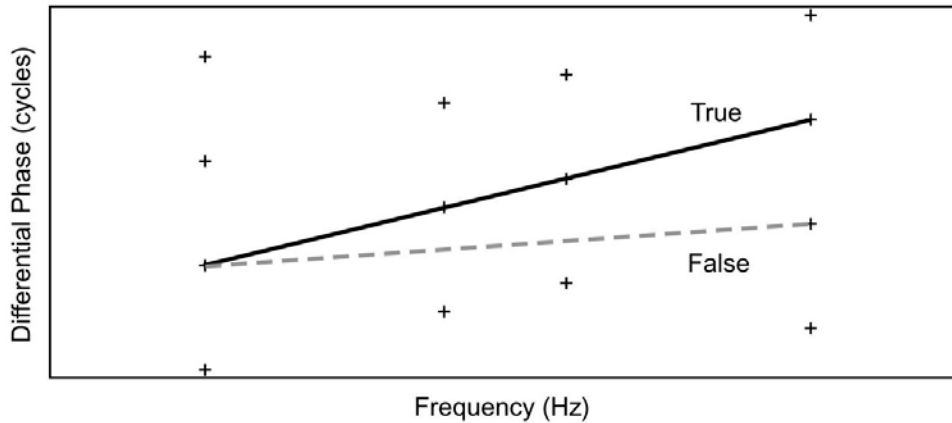

Figure 4. Resolution of Phase Ambiguity with a Second DOR Tone

It is important to use the largest possible spanned bandwidth because several measurement-limiting errors are inversely proportional to the spanned bandwidth. When selecting DOR tone frequencies, however, it is necessary to consider the problem of ambiguity resolution. Ambiguity resolution requires two signal components that are not widely separated in frequency. These two goals, achieving a large spanned bandwidth and resolving the ambiguity, are not contradictory. Generally, one DOR tone frequency is selected large enough that the desired measurement accuracy can be achieved. It will often be the case that the reciprocal of twice this frequency is smaller than the uncertainty in the *a priori* knowledge of differential group delay. This need not be a problem. The ambiguity can still be resolved by including one or more of the following in the measurement: a second (lower-frequency) DOR tone, the residual carrier, or telemetry subcarrier harmonics. The choice of how many signal components to use must be carefully considered because every signal that modulates the carrier consumes link power and produces intermodulation products that waste link power. These considerations are explored in Reference 4 and have been used to derive the recommendations in Reference 9.

2.4 ΔDOR Measurement Error Models

There are a number of important error sources for ΔDOR measurements. Precision for spacecraft delay depends on the power and spanned bandwidth of the DOR tones. Precision for quasar delay depends on the channel bandwidth and spanned bandwidth used to record the quasar signal. Instrumental error depends on clock stability, instrumental phase linearity, and spanned bandwidth. Errors in baseline length and orientation and errors in media delays scale with the angular separation between spacecraft and quasar. There is a natural trade-off between selecting a stronger source that might be at a larger angular separation from the spacecraft, or a weaker source that is angularly closer to the spacecraft. A denser radio source catalog provides more options to improve measurement geometry.

Section 3.4 of Reference 4 describes the significant error sources and gives quatitative models for estimating errors. Assumptions for model parameter values are presented that represent current DSN capabilities. The error budget presented in Reference 4 is summarized below in Paragraph 2.5 of this document. Section 4 of Reference 4 provides the trade-offs to consider when designing a measurement system and planning measurements.

It is important to note that these models are based on the assumption that the measurements are in fact ΔDOR, and not plain DOR. (Some of the following errors would be much larger for plain DOR, since common-mode errors would then not be canceled.) Units of time delay are employed here to characterize ΔDOR measurement error.

The errors of ΔDOR measurement can be dramatically reduced if a spacecraft defines the reference direction and if this reference spacecraft and the target spacecraft are close in an angular sense. If the two spacecraft are close enough to be observed simultaneously in common receive antennas, then this is called *Same-beam Interferometry*. Many of the error models discussed in Reference 4 and summarized below either do not apply or must be drastically modified for the case of Same-beam Interferometry. For more information on this technique and the errors associated with it, the reader may wish to see References 1 and 10.

2.5   Δ*DOR Measurement Error Budget*

An example error budget based on current DSN capability and good observing geometry is given here. Note that DSN observing geometry is generally good for spacecraft near the ecliptic plane, if the Sun-Earth-Spacecraft angle is greater than 10 deg, and either

(i)   observed from Goldstone-Canberra baseline; or

(ii)   geocentric angular declination above -15 deg and observed from Goldstone-Madrid baseline.

The 3-complex DSN has a geometric weakness when spacecraft are at far southern declinations. Delta-DOR cross-support from Agencies with antennas at other sites may be required to support highly accurate navigation for this case.

The assumptions used for the error budget are given in Table 7. The reader is referred to Reference 4 for context of these parameters. The ΔDOR error budget based on these assumptions is given in Table 8, showing both random and systematic effects. Table 8 provides 1-sigma error estimates that are representative of geometric and atmospheric conditions typically encountered with DSN ΔDOR measurements. The full error models provided in Reference 4 can be used to estimate the ΔDOR error for other conditions, geometries or assumptions.

For navigational analysis it is common to break out errors into random and systematic models. Table 9 shows only the random error components for ΔDOR, that is the random error in the difference between the spacecraft and quasar delay measurements. The root-sum-square (RSS) random error is less than 0.06 ns, corresponding to an angular error of 1.9 nrad on an 8000 km baseline. This angular error projects to a cross-position error of 281 m in the plane-of-sky at a distance of 1 AU.

There are known systematic errors that affect all radiometric data types. It is common for navigation analysis software to include explicit models and parameters for systematic effects. Table 10 shows parameters based on current DSN capability, for systematic error models in common use. If ΔDOR data are used for estimation purposes, and these systematic effects are explicitly included in the analysis, then only the random error component should be used for deriving the ΔDOR data weight.

The DSN ΔDOR system performed very well for the Mars Science Laboratory cruise phase and final approach to Mars. The root-mean-square (RMS) of the ΔDOR residuals to the final reconstructed trajectory was 0.038 ns (Reference 11).

Table 7. Nominal Parameter Values for Evaluation of X-band ΔDOR Error Budget

Term	Description	Nominal Value
T_{QU}	Total quasar observation time	960 s
T_{SC}	Total spacecraft observation time	480 s
$\Delta\theta$	Angular separation between spacecraft and quasar	0.1 rad
$\Delta\theta_B$	Component of spacecraft-quasar angular separation in direction of baseline projection	0.1 rad
γ_{SC_i}	Spacecraft elevation angle at station i	20 deg
γ_{QU_i}	Quasar elevation angle at station i	25 deg
SEP	Minimum angle between Sun and spacecraft or quasar	20 deg
f_{BW}	Spanned bandwidth	38.25×10^6 Hz
$(G/T)_i$	G/T for antenna i	52.56 dB K^{-1}
D	Channel sampling rate	16×10^6 samples/s
S_c	Quasar correlated flux density	0.4 Jy
K_L	System loss factor	0.8
k	Boltzman constant	1.38×10^{-23} Joules/K
λ	Radio Frequency wavelength	0.0356 m
SNR_{QU}	Quasar voltage SNR (derived)	261
P_{tran}	Effective transmitted tone power	108 Watts
R	Distance from spacecraft to receiver	150×10^9 m
FL	Spacecraft tone flux (derived)	3.981×10^{-22} W/m^2
$\left(P_{DOR}/N_0\right)_i$	DOR tone power to noise spectral density, station i (derived)	27 dB•Hz

Term	Description	Nominal Value
SNR_{SC_i}	Spacecraft voltage SNR (derived)	695
$T_{SC\text{-}QU}$	Time between centers of spacecraft and quasar scans	600 s
$\varepsilon_{\Delta f/f}$	Instrument frequency stability at 600 s	10^{-14}
ε_ϕ	Instrument phase ripple (nonlinearity across channel of few MHz bandwidth)	0.2 deg
ε_{BL}	Baseline coordinate uncertainty, each component	0.02 m
ε_{UTPM}	Baseline orientation uncertainty, each component (1 day prediction)	0.02 m
$\rho_{z_{wet_i}}$	Zenith wet troposphere delay uncertainty, station i	0.005 m
$\rho_{z_{dry_i}}$	Zenith dry troposphere delay uncertainty, station i	0.002 m
$\rho_{trop_{fluct}}$	Fluctuating troposphere uncertainty for 10 deg separation	0.01 m
$\rho_{iono_{day_i}}$	Daytime ionosphere model uncertainty (X-band level), station i	0.04 m
$\rho_{iono_{night_i}}$	Nighttime ionosphere model uncertainty (X-band level), station i	0.01 m
$\rho_{iono_{fluct}}$	Fluctuating ionosphere uncertainty for 10 deg separation (increase by $\times 2$ near solar max)	0.01 m
f_{RF}	Signal Radio Frequency	8.42 GHz
B_s	Separation of raypaths from radio source to two stations, at plane of signal closest approach to Sun	6×10^6 m
v_{SW}	Solar wind velocity	4×10^5 m/s
ε_g	Quasar coordinate uncertainty	0.75×10^{-9} rad
B_p	Length of baseline projection onto plane-of-sky	8×10^6 m

Table 8. Delta-DOR Error Budget (1 Sigma)—Both Random and Systematic Effects

Component	Random/Systematic	Delay Error (ns)
Quasar thermal noise	Random	0.023
Spacecraft thermal noise	Random	0.012
Clock instability	Random	0.006
Dispersive phase	Random	0.029
Station location	Systematic	0.007
Earth orientation	Systematic	0.007
Zenith troposphere	Systematic	0.012
Fluctuating troposphere	Random	0.019
Ionosphere shell	Systematic	0.019
Fluctuating ionosphere	Random	0.019
Solar plasma	Random	0.006
Quasar coordinate	Systematic	0.020
RSS total		**0.057**

Table 9. Delta-DOR Error Budget (1 Sigma)—Random Effects Only

Component	Delay Error (ns)
Quasar thermal noise	0.023
Spacecraft thermal noise	0.012
Clock instability	0.006
Dispersive phase	0.029
Fluctuating troposphere	0.019
Fluctuating ionosphere	0.019
Solar plasma	0.006
RSS random	**0.048**

Table 10. Common Parameters for Modeling Systematic Effects (1 Sigma)

Component	**Model Error**
Station Location[*]	2 cm with correlations
Earth Orientation	
UT1 1-day prediction	2 cm
UT1 after the fact	1 cm
Polar Motion	1 cm
Zenith Troposphere	
Wet	0.5 cm
Dry	0.2 cm
Ionosphere Shell	
Day (X-band level)	4 cm
Night (X-band level)	1 cm
Quasar Coordinate	0.75 nrad
[*]Correlations among station coordinates may be accounted for in a covariance matrix.	

Appendix A
DSN Document 810-005

Module 101, 70-m Subnet Telecommunications Interfaces

Module 103, 34-m HEF Subnet Telecommunications Interfaces

Module 104, 34-m BWG Antennas Telecommunications Interfaces

Module 106, Solar Corona and Solar Wind Effects

Module 107, X-band Radio Source Catalog

Module 203, Sequential Ranging

Module 214, Pseudonoise and Regenerative Ranging

Module 301, Coverage and Geometry

References

1. C. L. Thornton and J. S. Border, *Radiometric Tracking Techniques for Deep-Space Navigation*, Wiley-Interscience, Hoboken, NJ, 2003.

2. P. G. Antreasian, *et al*., "2001 Mars Odyssey Orbit Determination During Interplanetary Cruise," *AIAA/AAS Astrodynamics Specialist Conference and Exhibit*, Monterey, CA, August 5-8, 2002.

3. David W. Curkendall and James S. Border, "Delta-DOR: The One-Nanoradian Navigation Measurement System of the Deep Space Network — History, Architecture, and Componentry," The Interplanetary Network Progress Report, vol. 42-193, Jet Propulsion Laboratory, Pasadena, California, pp. 1-46, May 15, 2013.

    https://ipnpr.jpl.nasa.gov/progress_report/42-193/193D.pdf

4. *Delta-DOR -- Technical Characteristics and Performance*, Report Concerning Space Data System Standards, CCSDS 500.1-G-1, Green Book, Issue 1. Washington, D.C.: CCSDS, May 2013.

    https://public.ccsds.org/Pubs/500x1g1.pdf

5. C. Ma, Chairman, "The Second Realization of the International Celestial Reference Frame by Very Long Baseline Interferometry," IERS Technical Note No. 35, Verlag des Bundesamts fur Kartographie und Geodasie, Frankfurt am Main 2009.

6. C. Jacobs, *et al.*, "The JPL Extragalactic Radio Reference Frame: Astrometric Results of 1978-96 Deep Space Network VLBI," *TMO Progress Report 42-133*, Jet Propulsion Laboratory, Pasadena, CA, May 15, 1998.

    https://ipnpr.jpl.nasa.gov/progress_report/42-133/133E.pdf

7. T. P. McElrath, W. M. Watkins, B. M. Portock, E. J. Graat, D. T. Baird, G. G. Wawrzyniak, A. A. Attiyah, J. R. Guinn, P. G. Antreasian, R. C. Baalke, and W. L. Taber, "Mars Exploration Rovers Orbit Determination Filter Strategy," AIAA-2004-4982, paper presented at the AIAA/AAS Astrodynamics Conference, Providence, Rhode Island, August 15-20, 2004.

8. Shervin Shambayati, David Morabito, James S. Border, and Faramaz Davarian, Mars Reconnaissance Orbiter Ka-Band Demonstration: Cruise Phase Operations, Chapter 15 in Space Operations: Mission Management, Technologies, and Current Applications, Edited by Loredana Bruca, J. Paul Douglas, Trevor Sorensen, Progress in Astronautics and Aeronautics, Frank K. Lu, Editor-in-Chief, Volume 220, American Institute of Aeronautics and Astronautics, Inc., Reston, Virginia, 2007.

9.   *Radio Frequency and Modulation Systems—Part 1: Earth Stations and Spacecraft*, Recommendation for Space Data System Standards, CCSDS 401.0-B-24, Blue Book, Issue 24, Washington, D.C.: CCSDS, October 2014.

     https://public.ccsds.org/Pubs/401x0b29.pdf

10. J. S. Border, *et al*., "Precise Tracking of the Magellan and Pioneer Venus Orbiters by Same-Beam Interferometry, Part I: Data Accuracy Analysis," *TDA Progress Report 42-110*, Jet Propulsion Laboratory, Pasadena, CA, August 15, 1992.

     https://ipnpr.jpl.nasa.gov/progress_report/42-110/110A.PDF

11. T. J. Martin-Mur, G. L. Kruizinga, P. D. Burkhart, F. Abilleira, M. C. Wong, and J. A. Kangas, "Mars Science Laboratory Interplanetary Navigation," *Journal of Spacecraft and Rockets*, Vol. 51, Issue 4, pp. 1014-1028, July 2014.